metals

MDPI

Article

Effects of Borax and Grinding Alkalinity on the Reduction–Magnetic Separation of Beach Placer

Bing Hu [1], Peiwei Hu [2,3,*], Runqin Gao [2], Chao Hu [2,4] and Fuqiang Zheng [1]

[1] National Engineering Research Center of Sintering and Pelletizing Equipment System, Zhongye Changtian International Engineering Co., Ltd., Changsha 410205, China
[2] College of Resources and Environment Engineering, Wuhan University of Science and Technology, Wuhan 430081, China
[3] Hubei Key Laboratory for Efficient Utilization and Agglomeration of Metallurgic Mineral Resources, Wuhan University of Science and Technology, Wuhan 430081, China
[4] Suzhou Sinoma Design & Research Institute of Non-Metallic Minerals Industry Co., Ltd., Suzhou 215151, China
* Correspondence: pwhu@wust.edu.cn; Tel.: +86-27-6886-2204

Abstract: The effect of borax on the reduction characteristics of Indonesia beach placers was investigated. The effect of grinding alkalinity on the magnetic separation of the reduced sample was also studied in this paper. The mineral phase transformation, microstructures of reduction, and magnetic separation products were analyzed to reveal the enhanced separation mechanism of titanium and iron in beach placer. The borax could effectively improve the metallization rate and the growth of iron grains in a reduced sample. When 3% borax was added to the reduction process, the metallization rate of the reduced beach placer reached 95.64%, and the metal iron grains grew to about 50 μm. Adjusting the grinding alkalinity could prevent the metallic iron from being oxidized and promote the monomer dissociation between mineral particles. The iron powder concentrates with 94.07% total Fe and vanadium-rich titanium slag with 36.32% Ti were obtained by grinding magnetic separation as the grinding alkalinity pH was 13.

Keywords: beach placer; borax; enhanced reduction; mill alkalinity; metallization rate

Citation: Hu, B.; Hu, P.; Gao, R.; Hu, C.; Zheng, F. Effects of Borax and Grinding Alkalinity on the Reduction–Magnetic Separation of Beach Placer. *Metals* **2023**, *13*, 868. https://doi.org/10.3390/met13050868

Academic Editor: Fernando Castro

Received: 20 March 2023
Revised: 21 April 2023
Accepted: 24 April 2023
Published: 29 April 2023

1. Introduction

Sea placer is a mineral dominated by ilmenite solid solution, which is usually formed in rapidly cooled volcanic lava, so it is mostly concentrated in coastal areas, such as New Zealand, Indonesia, South Africa, and the South China Sea [1]. Beach placer is a kind of multi-metal co-associated ore with iron, titanium, and vanadium elements as the main symbiosis as well as other useful elements (cobalt (Co), nickel (Ni), chromium (Cr), copper (Cu), etc.), which are widely spread all over the world and rich in reserves [2]. Beach placer is internationally recognized as a strategic mineral due to its multi-metallic content [3,4]. Beach placer is highly weathered, with a large Fe_2O_3/FeO ratio and high Ti content, while Ti-bearing material often exists in the form of ilmenite ($FeTiO_3$), ulvospinel (Fe_2TiO_4), and titanium magnetite ($Fe_{3-x}Ti_xO_4$) [5,6]. Due to the close symbiosis of Fe and Ti elements from beach placer, the methods of separating them efficiently have become a hot issue in current research [7]. Until now, numerous studies were conducted for this kind of complex minerals, such as the pre-reduction–electric furnace method [8,9], sodium vanadium extraction–pre-reduction–electric furnace method [10,11], and reduction–grinding method [12,13]. The reduction–grinding method became the most common process method in beach placer smelting due to its high metal rate of the product and achievement of separation of Fe, Ti, and V [14]. The key is to change the structure of the minerals during the reduction roasting stage, so that the Fe and Ti elements can be separated, migrated, and enriched, thus realizing efficient separation [15].

In the reduction roasting stage, additives can enhance reduction and improve the separation of elements [16,17]. The additives utilized in the reduction roasting stage of titanium ore are generally classified into three main categories. The first is to improve the lattice distortion energy of minerals, such as Na_2CO_3 and other alkali metal salts [18]. The second is to accelerate the atomic transport during the reduction process, such as boron sand and other boron-bearing additives [11]. The last is to provide heat of reaction, such as ferrosilicon [19]. Agrawal et al. [20] used microwave irradiation to produce submicron cracks in iron sulfate (III) and oxidized titanium sulfate particles, which could increase the intergranular gap of the minerals and the degree of monomer dissociation, facilitating the subsequent separation of iron and scandium along with the roasting process. Yao et al. [19] studied the influence of various parameters on the preparation of reduced iron powder. The results showed that pyrite was the optimal additive that formed a molten iron sulfide (FeS) phase. Spheroidal metallic iron particles were more easily encapsulated by the FeS phase, which was more conducive to the separation of metallic iron and oxide impurities. Studies have shown that grinding conditions are also an important factor affecting magnetic separation, and there are few studies on pulp alkalinity. This paper explores experiments and finds that pulp alkalinity is an important indicator affecting magnetic separation. Thus, a simple direct reduction magnetic separation has been difficult to meet the requirements of the vanadium titanomagnetite separation process, so the modern process prefers to use a combination of various processes [21].

At present, there are few studies on the comprehensive utilization of sea sand resources. Therefore, the mechanism of beach placer reduction by microwave heating was studied, with emphasis on the effect of borax on the transformation of Ti–Fe-bearing minerals. Moreover, the mechanism of grinding magnetic separation of reduced beach placer was also investigated in the present work focusing on the effect of grinding alkalinity on the magnetic separation of Ti and Fe. It provides a theoretical basis for the development of new processes and technologies for the comprehensive utilization of titanium magnetite.

2. Materials and Method

2.1. Materials

The beach placer was obtained from Indonesia. The composition of the beach placer, as examined by chemical titration, is presented in Table 1, which showed that the total iron content in the ore is 54.27%. The iron element is mainly present in the form of Fe^{3+} and Fe^{2+} in the mineral, and its mass fractions are calculated to be 31.65% and 22.62%, respectively. X-ray diffraction was used to qualitatively analyze the beach placer, and mineral monomer dissociation analysis (MLA) was used to quantitatively analyze the mineral content. The main mineral content is shown in Table 2. It can be seen from Tables 1 and 2 that the beach placer is a kind of vanadium titanium magnetite, which meets the quality standard of first-grade iron concentrate ($S \leq 0.1\%$, $p \leq 0.2\%$). It is necessary to separate and recover Fe, Ti, and other metals.

Table 1. Main chemical compositions of beach placer/wt.%.

FeO	Fe_2O_3	TiO_2	V_2O_5	SiO_2	Al_2O_3	CaO	MgO	MnO	Na_2O	K_2O	S	P	LOI *
29.08	45.21	10.88	0.68	4.01	3.67	0.48	3.68	0.44	0.93	0.21	0.06	0.03	0.64

* LOI-loss on ignition.

Table 2. Main mineral content of beach placer/wt.%.

Mineralogical Phases	Titanomagnetite	Haplotypite	Ilmenite	Pyroxene
content/%	83.21	6.93	1.87	5.61

The industrial analysis of biomass char as a reductant is shown in Table 3. The grinding alkalinity was regulated by adding NaOH solution. The additives (Na_2CO_3, CaF_2, $Na_2B_4O_7{\cdot}10H_2O$, and H_3BO_3) used in this work were all analytical reagents.

Table 3. Industrial analysis of biochar/wt.%.

Reductant	Moisture	Fixed Carbon	Volatile Fraction	Ash
biochar	6.51	80.81	15.65	3.54

2.2. Experimental Method

The experiments were mainly divided into three parts: raw material pre-treatment, reduction roasting, and reduced sample grinding separation. The experiment flow is shown in Figure 1. The pre-treatment of beach placer is mainly done by pre-oxidation. The specific steps are as follows: 500 g beach placer was distributed in a vertical microwave heating furnace, and the microwave generator generated a microwave with a fixed power of 7 kW. During the test, the air was continuously introduced and reacted with the minerals. The airflow was fixed at 1 L/min, the pre-oxidation temperature was 1050 °C, and the constant temperature was held for 90 min to ensure that the beach placer was fully oxidized; the titanium magnetite was oxidized to titanium hematite as much as possible. After the pre-oxidation treatment was completed, the material was taken out and placed in the air to cool naturally to room temperature, weighed, and stored.

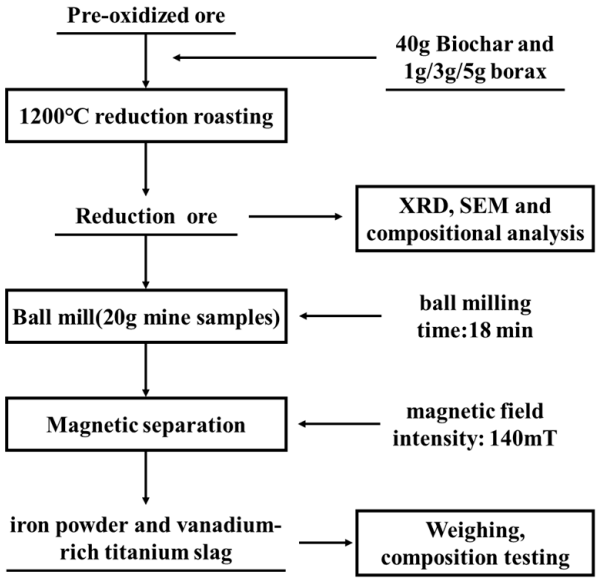

Figure 1. Process flow diagram.

In the reduction roasting stage, the pre-oxidized ore, biomass carbon, and additives were mixed in a certain mass ratio (carbon to iron ratio of 0.6, different additives, such as Na_2CO_3, CaF_2, $Na_2B_4O_7{\cdot}10H_2O$, and H_3BO_3, were used to investigate the effect of additives on reduction and separation of beach placer. The dosage was 3%.). The mixed powder was put into a φ7 cm × H 15 cm mullite crucible, which was sealed with insulation cotton. Then the crucible was placed in a microwave furnace to reduce at 1200 °C for 100 min. The microwave heating power range, and heating rate of the microwave furnace were 0−9000 W and 28 °C/min, respectively. The schematic diagram of the microwave furnace is shown in Figure 2. After the reduction experiment, the reduced sample was cooled to room temperature in an N_2 atmosphere.

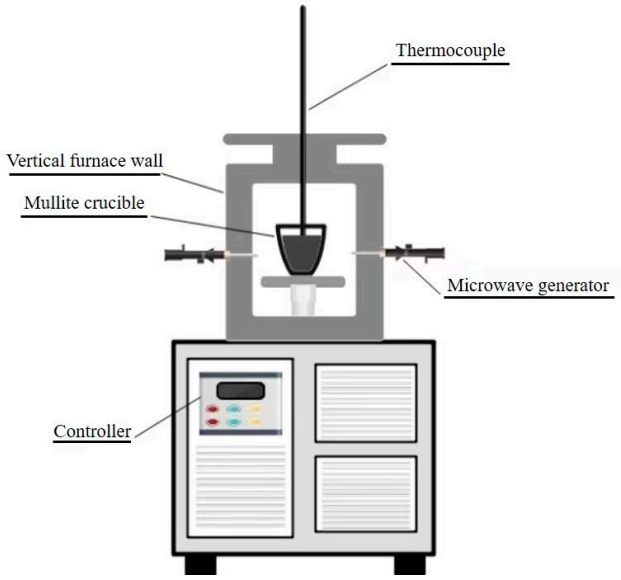

Figure 2. Schematic diagram of microwave furnace.

The step of reduced sample grinding and separation: 20 g of reduction sample was ground by a conical ball mill (XMQ type 240*90) with a pulp concentration of 50% for 18 min. The effect of grinding alkalinity on the magnetic separation of iron and titanium was investigated. NaOH solution was added to adjust the grinding slurry pH to 10, 11, 12, 13, and 14. Concomitantly, the concentration of Fe, Si, and Ti ions in the slurry supernatant was measured. The grinding pulp was separated by a magnetic separation tube (XCGS type Φ50) at 140 mT. The iron powder concentrate and vanadium-rich titanium slag were obtained for chemical composition and microstructure analysis.

The metallization rate of the reduction product was defined as Equation (1).

$$\text{metallization rate}(\eta) = \frac{MFe}{TFe} \times 100\% \quad (1)$$

where η was the metallization rate of the reduction product (%), *MFe* was the metallic iron content of the reduction product (%), and *TFe* was the total iron content of the reduction product (%).

The main evaluation index of the grinding test was the grade or recovery of *TFe* and TiO_2 from iron powder and vanadium-titanium slag. The contents of *TFe* and TiO_2 were derived from the chemical analysis, and the formulas for recovery are shown in Equations (2) and (3).

$$\mu = \frac{m_1 \times \alpha_1}{m_0 \times TFe} \times 100\% \quad (2)$$

$$\xi = \frac{m_2 \times \beta}{m_0 \times \delta} \times 100\% \quad (3)$$

where μ was the iron recovery rate (%), m_1 was the weight of iron powder (g), α_1 was the mass fraction of total iron in the iron powder, and m_0 was the weight of the return material from grinding (g). The ξ was the TiO_2 recovery rate in the vanadium-rich titanium slag (%), m_2 was the weight of TiO_2 in the vanadium-rich titanium slag (g), β was the mass fraction of TiO_2 in the vanadium-rich titanium slag (%), and δ was the mass fraction of TiO_2 in the returned raw material (%).

2.3. Characterization of Minerals

The industrial analyzer (SDTGA-5000, Changsha Sande Industrial Co., Ltd. Changsha, China) was used to determine the chemical composition of biochar; the microscopic morphology of the minerals was analyzed by scanning electron microscopy (JSM-IT500LV, JEOL Ltd., Tokyo, Japan) and SEM energy-dispersive X-ray spectroscopy (EDS); the phase transformation of minerals was studied by X-ray diffractometer (Advance D8, Bruker, Mannheim, Germany). The particle size distribution of minerals was studied by a laser particle size analyzer (MS2000 Malvern, Malvern, UK). The pH meter tester (PHS-3C, Shanghai LeiMagnetic Instrument Co., Ltd., Shanghai, China) was used to determine the pulp alkalinity of grinding.

3. Results and Discussion

3.1. Effects of Borax on the Reduction–Grinding–Magnetic Separation of Beach Placer

The effect of additives on the reduction separation of beach placer is shown in Figure 3. It can be seen from Figure 3a that the metallization rate of the reduced sample without additives was 92.42%. After adding borax, the metallization rate reached 95.64%, which was the highest among all additives. Figure 3b,c showed the effect of additives on magnetic separation indexes of the reduced sample. The separation of Ti–Fe of the reduced sample with borax was significantly improved in process of grinding and magnetic separation. The iron grade and iron recovery rate of iron powder concentrate were 86.23% and 98.10%, respectively. The grade of TiO_2 in vanadium-rich titanium slag was also up to 33.5%, and the recovery rate of TiO_2 was 54.14%. Therefore, borax was used as a reduction additive for subsequent research.

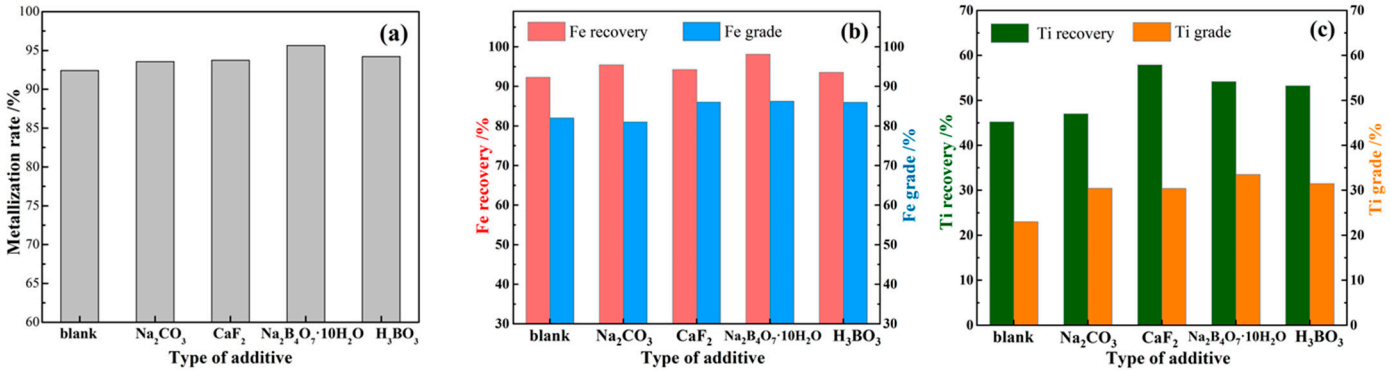

Figure 3. Effects of additives on the reduction–grinding–separation of beach placer: (**a**) the metallization rate, (**b**) the recovery and grade of Fe, and (**c**) the recovery and grade of Ti.

To further investigate the effect of borax on the reduction characteristics of beach placer, the reduction roasting of beach placer with different borax dosages was studied. As shown in Figure 4a, the metallization rate increased from 92.42% to 95.64% with the increase of borax dosage from 0% to 3%. It can be seen from Figure 4b that the iron grade in iron powder concentrate increased first and then decreased with increasing borax dosage, which corresponded to the change in metallization rate. When the borax dosage was 3%, the iron grade and iron recovery rate reached the maximum values, which were 86.23% and 98.10%, respectively. Moreover, the iron grade and iron recovery rate decreased by 0.37% and 5.06%, respectively, when the borax dosage was up to 5%. The recovery rate of TiO_2 in vanadium-rich titanium slag increased with the increase of borax, as shown in Figure 4c. The TiO_2 grade of vanadium-rich titanium slag reached the highest value when the dosage of borax was 3%. Therefore, adding 3% borax in the beach placer during reduction roasting was beneficial to the efficient separation of Ti–Fe.

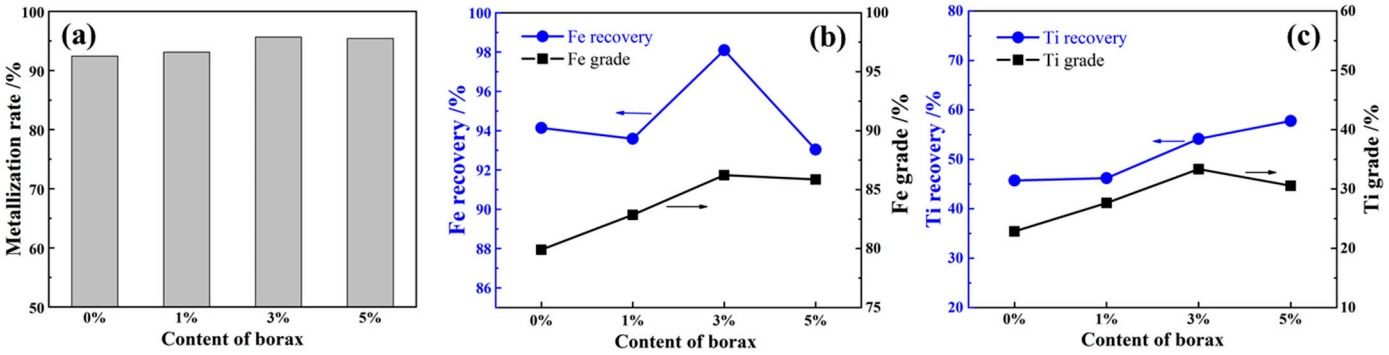

Figure 4. Effects of borax dosage on the reduction–grinding–separation of beach placer: (**a**) the metallization rate, (**b**) the recovery and grade of Fe, and (**c**) the recovery and grade of Ti.

The reduction path for iron oxides in beach placer was $Fe_2O_3 \rightarrow Fe_3O_4 \rightarrow FeO \rightarrow Fe$ [22], and for titanium-containing oxides, it was $Fe_2TiO_4 \rightarrow FeTiO_3 \rightarrow FeTi_2O_5 \rightarrow TiO_2$ [23,24]. A small amount of iron in the form of iron $FeO{\cdot}SiO_2$, $FeO{\cdot}Al_2O_3$, and Fe_2SiO_4 in beach placer is difficult to be reduced. Since borax ($Na_2B_4O_7$) could dissociate Na_2O at 1150 °C, then Na_2O would combine with SiO_2 and Al_2O_3 to replace FeO and promote the transformation from FeO to Fe, which could improve the metallization rate of the reduced product. The reaction equations are shown in Equations (4)–(6) [25].

$$2FeO{\cdot}SiO_2 + Na_2O \rightarrow Na_2O{\cdot}SiO_2 + 2FeO \quad (4)$$

$$FeO{\cdot}Al_2O_3 + Na_2O \rightarrow Na_2O{\cdot}Al_2O_3 + FeO \quad (5)$$

$$2Fe_2SiO_4 + FeO{\cdot}Al_2O_3 + Na_2O \rightarrow Na_2O{\cdot}Al_2O_3{\cdot}2SiO_2 + 5FeO \quad (6)$$

In addition, the borax additive contained the $[BO_3]$ atomic group, B^{3+} attracted the valence electron cloud of Si–O–Si in the reduction roasting process, which led to the breakage of some Si–O–Si bonds. And then caused the separation of the SiO_2 and FeO, which promoted the transformation of FeO to Fe. However, when additional amount of borax was higher than 3%, the Na-bearing solid solutions and B-bearing solid solutions with low melting points were increased, which lead to the increase of the liquid phase in the sample during reduction roasting [26]. The liquid phase encapsulated the surface of the iron ore is reduced and blocked the channel of the reducing gas and hindered the further reduction reaction.

3.2. Effects of Borax on the Mineral Phases of Reduced Products

Figure 5 showed that the Ti-bearing mineral phases between the reduced samples without borax and the original ore were the same, which were still in close symbiosis with Fe [27]. After adding borax, Fe was separated from Ti, and the relative intensity of the iron diffraction peak increased. Borax promoted the conversion of FeO in $Fe_3Ti_3O_{10}$ to Fe. Meanwhile, the characteristic peaks of $Fe_3Ti_3O_{10}$ at 26° were converted to anatase and rutile TiO_2 peaks, respectively, which was because part of $Fe_3Ti_3O_{10}$ was reduced to Fe and TiO_2. Therefore, borax not only helped the reduction of the iron-bearing phase to Fe, but also promoted the separation between Fe and Ti.

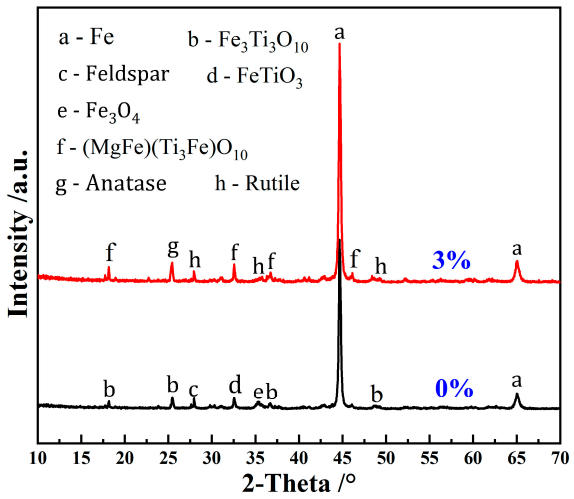

Figure 5. XRD patterns of the reduced products without and with borax.

3.3. Effects of Borax on the Microstructure of Reduced Products

The effect of borax addition on the microstructure of the reduced products is shown in Figure 6. It can be seen that the mineral of reduced products was mainly divided into three categories, which were the metallic iron with bright white, the titanium-rich mineral with dark gray, and the veinstone with black.

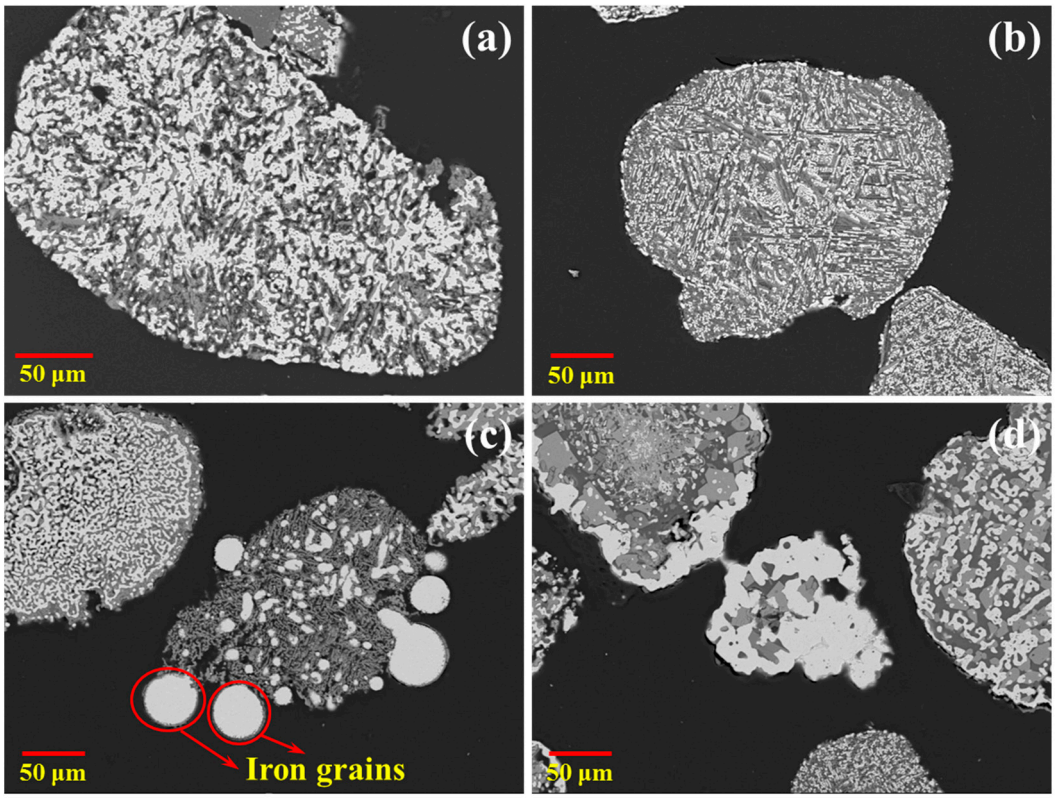

Figure 6. SEM images of the reduced products with different borax additions: (**a**) 0%, (**b**) 1%, (**c**) 3%, and (**d**) 5%.

When the borax dosage was lower than 3%, as shown in Figure 6a,b, there was no obvious change in the grain morphology of metallic iron. The titanium-rich mineral was closely embedded with metallic iron. The metallic iron was mostly in the form of thin strips with a width of less than 20 μm. However, when the borax dosage increased to 3%,

as shown in Figure 6c, the metal iron began to accumulate and grow. A large number of iron grains with a uniform spherical size of about 50 μm appeared at the edge of the reduced particles. In the reduced particles, there were also some aggregated metallic iron grains with a size of 10 μm. When the borax dosage increased to 5%, as shown in Figure 6d, metallic iron migrated to the outside of the particle and aggregated to wrap some titanium-rich minerals. The size of metal iron increased obviously, but the morphology was irregular. This phenomenon was mainly because the borax could decrease the melting point of reactants, while reducing the surface tension of iron grains, thereby promoting the accelerated diffusion of iron particles [28]. Therefore, adding an appropriate amount of borax during reduction progress was beneficial to promote the aggregation and growth of iron grains.

The reduced products with 3% borax were analyzed by EDS to study the elemental composition as shown in Figure 7. Most of the iron elements were aggregated into metallic iron particles alone, and few other elements were distributed in the metallic iron particles. Metal iron particles were granular, and the size was generally greater than 50 μm. There was a tendency of interconnection and aggregation between iron particles, which had no other impurity elements. The Ti was mainly distributed in the uniformly large fish-scale titanium-rich phase. Ca, Mg, Al, Na, and Si elements performed the same, and most of them existed in the veinstone mineral between the metallic iron and titanium-rich mineral. There was an obvious separation between the titanium-rich mineral and metallic iron. Therefore, there was a clear variability in the orientation of Ti and Fe elements. Fe appeared to be separated from Ti-bearing minerals in the reduction process. After reduction, Fe was enriched in the metallic iron grains and Ti was enriched in the titanium-rich mineral grains.

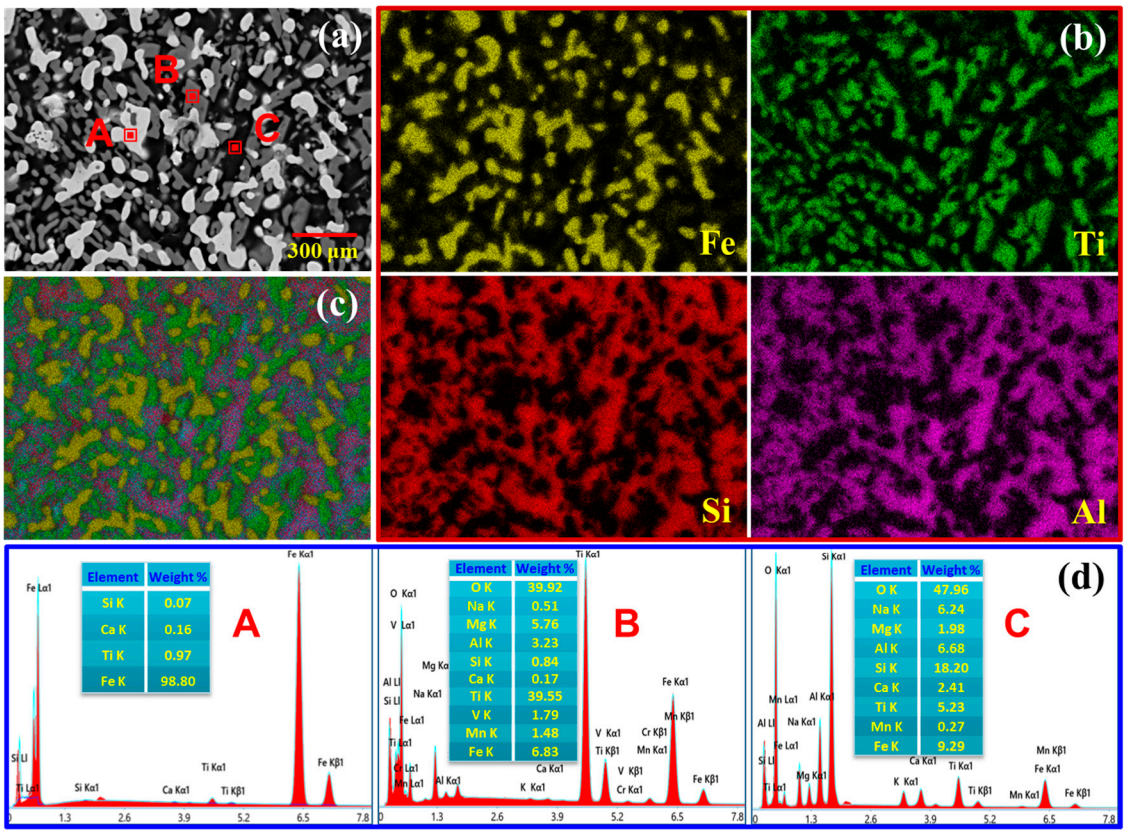

Figure 7. SEM image (**a**), and elemental mapping (**b**,**c**) and EDS spectrum (**d**) of reduced product.

Spectrum A was in the bright white material (Figure 7d). The mass fractions of iron, titanium, and calcium in spectrum A were 98.8%, 0.97%, and 0.16%, respectively. So, it indicated that the bright white material was mainly composed of metallic iron.

Spectrum B was in the gray-black scaly material growing at the edge of the bright white material. The main element in spectrum B was titanium with a mass fraction of 39.55%. Compared to the bright white material at this location, the mass fraction of iron was only 6.83%. The contents of vanadium, magnesium, aluminum, and oxygen were 1.79%, 5.76%, 3.23%, and 39.92%, respectively. It was known that the titanium element was mainly present in the solid solution of titanium-rich and magnesium (iron)-bearing black titanite ($(Fe,Mg)Ti_2O_5$) at this site. Spectrum C was in the black material in the gap between bright white and gray material. The mass fraction of silicon increased significantly to 18.2% compared to graphs A and B. It was known from the previous section that the sodium ion in borax would dissociate into Na_2O and then combine with SiO_2 and Al_2O_3 at 1200 °C under the reduction atmosphere. Therefore, the mass fraction of sodium element at this place was comparable to that of Fe and Ti at 6.24%. It also contained a certain amount of Ca, Mg, and Al, indicating that the region was mainly composed of O, Si, Al, Ca, and Mg complex compounds.

3.4. Effects of Borax on the Microstructure of Vanadium-Rich Titanium Slag

The SEM analysis of the vanadium-rich titanium slag obtained by grinding and separating the reduced sample with different borax additions is shown in Figure 8. It illustrated that the increase of borax was beneficial to reduce the appearance of metallic iron particles in the vanadium-rich titanium slag. When the borax dosage was less than 3%, a more metallic iron phase presented in the titanium-rich phase. When the borax dosage increased to 5%, there was more non-magnetic material. This phenomenon would reduce the TiO_2 content in the vanadium-rich titanium slag, while the excessive amount of alkali metal would harm the environment and subsequent industrial utilization of titanium sponges. Therefore, the optimal reduction conditions were a borax dosage of 3%, reduction temperature at 1200 °C, and reduction time of 90 min.

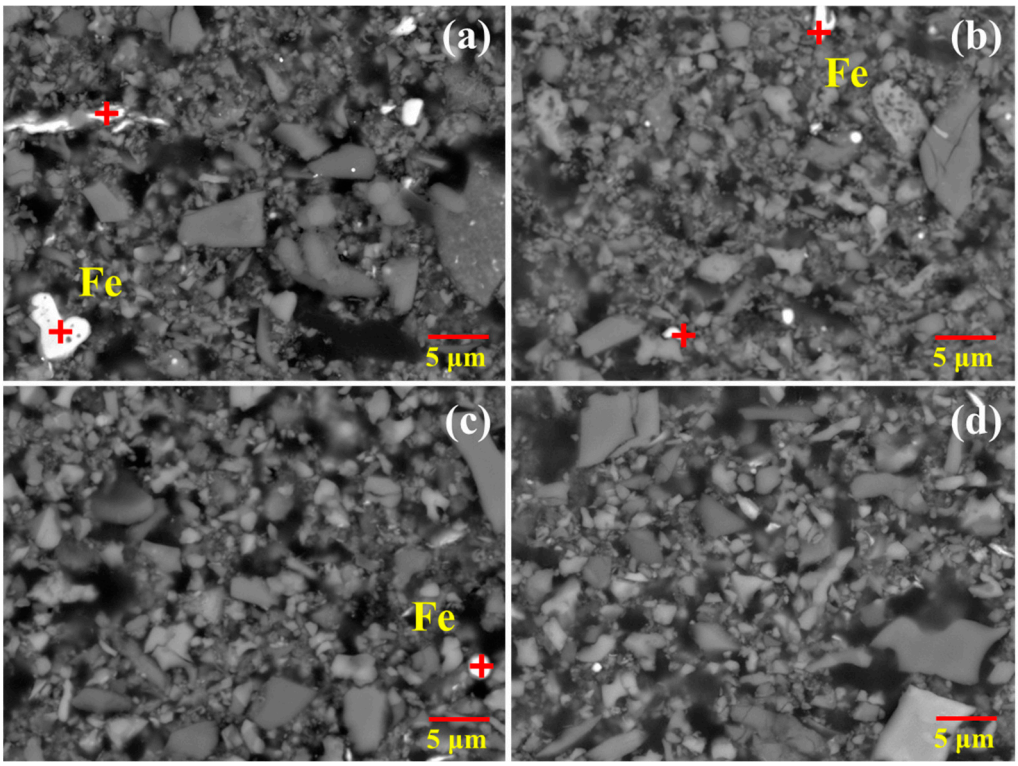

Figure 8. SEM images of the separated products with different borax additions: (**a**) 0%, (**b**) 1%, (**c**) 3%, and (**d**) 5%.

3.5. Effect of Grinding Alkalinity on Magnetic Separation and the Mechanism

The magnetic separation conditions were also important parameters that affected the elements' efficient separation [29,30]. The effect of grinding alkalinity on the Fe and Ti separation under the magnetic separation conditions of ball milling time at 18 min and magnetic field strength at 140 mT was investigated. As shown in Figure 9, the pH had little effect on Fe recovery and Ti grade. When the pH was raised from 11 to 14, both Fe grade and Ti recovery showed a trend of first increasing and then decreasing. When the pH was 13, the Fe grade reached the highest value of 94.07% in Fe powder, and the highest TiO_2 recovery was 79.84% in titanium-rich slag.

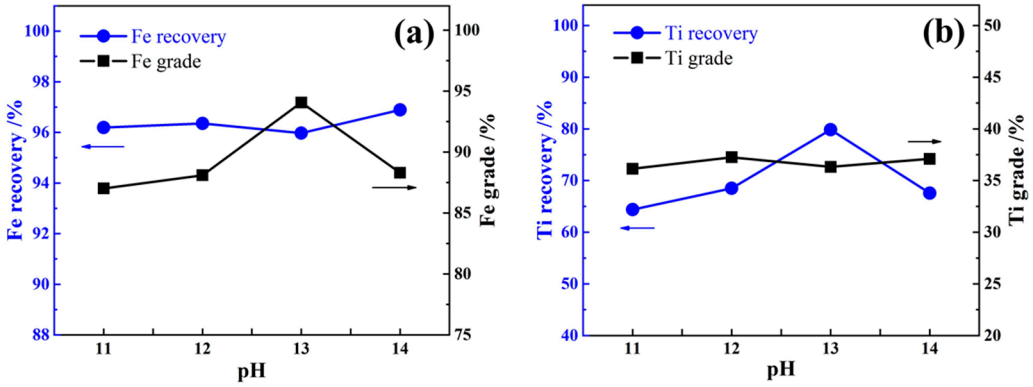

Figure 9. Effects of grinding alkalinity on Fe (**a**) and Ti (**b**) separation.

Figure 10 showed the effect of pH on the main ion concentration of the leaching solution. The Si ion concentration was much higher than that of Ti and Fe ions. When the pH was 11, the Si ion concentration in the leaching solution was 59.97 mg/L. The Si ion concentration increased with the increase of the pH. When the pH was 14, the Si ion concentration in the leaching solution reached 485.10 mg/L. Silicates were decomposed into soluble silicates in solutions with high OH^- concentrations. The Ti ion concentration was as low as 0.44 mg/L at pH = 13; meanwhile, the Fe ion concentration was as low as 0.93 mg/L. The results showed that when the pH was 13, the mineral structure was mostly destroyed, while reducing the loss of iron and titanium to improve Ti and Fe recovery.

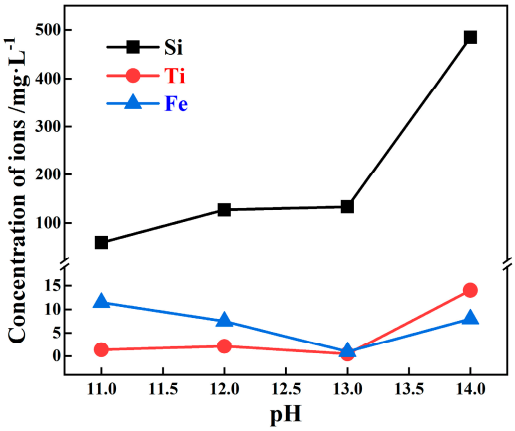

Figure 10. Effects of pH on main ion concentration of leaching solution.

XRD patterns of the vanadium-rich titanium slag obtained by grinding and separation at a different grinding alkalinity are shown in Figure 11. The main mineral in vanadium-rich titanium slag was anosovite ($Mg_xTi_{3-x}O_5$), followed by magnesia-alumina spinel, and trace amounts of pyroxene were also detected. The characteristic peaks of calcite appeared at 29°, 43°, and 47° in the vanadium-rich titanium slag samples when the pH was 13 [31]. The reduced sample was more easily dissociated monomerically when the pH reached 13.

The calcite connected with metallic iron was broken and finally entered the vanadium-rich titanium slag through magnetic separation.

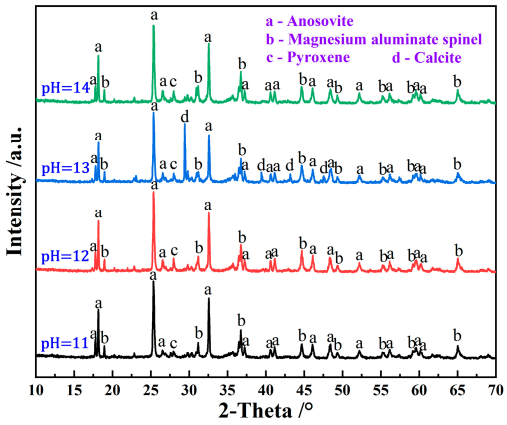

Figure 11. XRD of vanadium-rich titanium slag at different pH values.

Figure 12 showed the SEM images of the vanadium-rich titanium slag obtained by grinding and separation under different grinding alkalinity conditions. A thin film appeared on the surface of metallic iron particles with the pH increasing from 11 to 13, because metallic iron was prone to generate an Fe $(OH)_3$ passivation protective layer under an alkaline environment. It could prevent the metallic Fe from being further oxidized to Fe_2O_3 in the magnetic separation process after grinding. Meanwhile, the surface of gangue mineral particles had already been eroded. Some gangue minerals reacted with OH^- in the alkaline environment, which led to the insoluble mineral impurities entering the solution. Therefore, the grade of TiO_2 in the vanadium-rich titanium slag was improved by dissolving the gangue minerals into pulp.

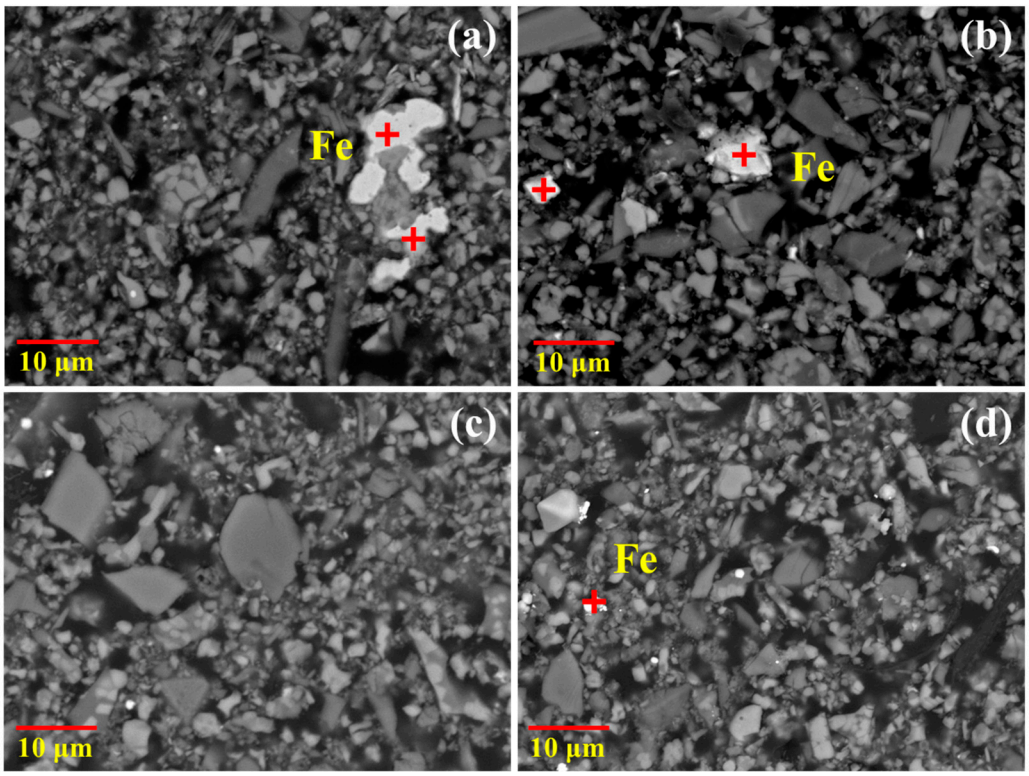

Figure 12. SEM images of vanadium-rich titanium slag obtained by grinding and sorting at different pH values: (**a**) pH = 11, (**b**) pH = 12, (**c**) pH = 13, and (**d**) pH = 14.

4. Conclusions

The borax could effectively improve the metallization rate of the reduction product. The metallization rate of reduced beach placer with 3% borax reached 95.64%. At this time, the metal iron grains in the reduced beach placer deposits accumulated and grew to about 50 μm. The main mineral phases in the reduced products with 3% borax were divided into three categories: metallic iron phase, titanium-rich phase, and veinstone phase. The metallic iron phase contained 98.80% Fe and 0.97% Ti, while the titanium-rich phase contained 39.55% Ti and 6.83% Fe. Borax significantly promoted the separation of Ti and Fe in the reduction process. Adjusting the alkalinity in the grinding stage could also improve the magnetic separation efficiency of Fe and Ti. The best effect of the grinding separation was achieved at pH 13, where the Fe grade in Fe powder was 94.07% and Fe recovery was 95.97%, and the TiO_2 grade in vanadium-rich titanium slag was 36.32% and TiO_2 recovery was 79.84%.

Author Contributions: Conceptualization, B.H. and P.H.; methodology, B.H. and C.H.; data curation, C.H. and R.G.; writing—original draft preparation, R.G. and B.H.; writing—review and editing, F.Z. and P.H.; project administration, P.H. All authors have read and agreed to the published version of the manuscript.

Funding: This work was supported by Hunan Provincial Natural Science Foundation of China (2019JJ51007).

Data Availability Statement: Not applicable.

Conflicts of Interest: The authors declare no conflict of interest.

References

1. Turner, M.B.; Cronin, S.J.; Stewart, R.B.; Mark, B.; Smith, l.E.M. Using titanomagnetite textures to elucidate volcanic eruption histories. *Geology* **2008**, *36*, 31–34. [CrossRef]
2. Hu, Z.; Zhang, H.; Li, H.W.; Chen, Z.-Q.; Zhang, F.-H. Study on reasonable mineral processing flowsheet of a beach placer in Indonesia. *Min. Metall. Eng.* **2009**, *29*, 33–35.
3. Hu, T.Y.; Sun, T.C.; Kou, J.; Geng, C.; Wangm, X.; Chen, C. Recovering titanium and iron by co-reduction roasting of seaside titanomagnetite and blast furnace dust. *Int. J. Miner. Process.* **2017**, *165*, 28–33. [CrossRef]
4. Brathwaite, R.L.; Gazley, M.F.; Christie, A.B. Provenance of titanomagnetite in ironsands on the west coast of the North Island, New Zealand. *J. Geochem. Explor.* **2017**, *178*, 23–34. [CrossRef]
5. Samanta, S.; Mukherjee, S.; Dey, R. Oxidation behaviour and phase characterization of titaniferous magnetite ore of eastern India. *Trans. Nonferr. Met. Soc. China* **2014**, *24*, 2976–2985. [CrossRef]
6. Gunanto, Y.E.; Izaak, M.P.; Cahyadi, L.; Jobiliong, E.; Adi, W.A. Preliminary study: Local iron sand characterization of titanomagnetite type. *IOP Conf. Ser. Mater. Sci. Eng.* **2018**, *367*, 012059. [CrossRef]
7. Liu, J.S.; Xing, Z.X.; Cheng, G.J.; Xue, X.X.; Ding, X.Y. Study on the grinding kinetics and magnetic separation of low-grade vanadiferous titanomagnetite concentrate. *Metals* **2022**, *12*, 575. [CrossRef]
8. Wang, S.; Guo, Y.F.; Jiang, T.; Chen, F.; Zhen, F.-Q.; Tang, M.-J.; Yang, L.-Z.; Qiu, G.-Z. Appropriate titanium slag composition during smelting of vanadium titanomagnetite metallized pellets. *Trans. Nonferr. Met. Soc. China* **2018**, *28*, 2528–2537. [CrossRef]
9. Jiang, T.; Wang, S.; Guo, Y.F.; Chen, F.; Zheng, F. Effects of basicity and MgO in slag on the behaviors of smelting vanadium titanomagnetite in the direct reduction-electric furnace process. *Metals* **2016**, *6*, 107. [CrossRef]
10. Li, G.H.; Zhang, S.H.; Rao, M.J.; Zhang, Y.B.; Jiang, T. Effects of sodium salts on reduction roasting and Fe-P separation of high-phosphorus oolitic hematite ore. *Int. J. Miner. Process.* **2013**, *124*, 26–34. [CrossRef]
11. Li, Y.L.; Qu, J.K.; Wei, G.Y.; Qi, T. Influence of Na_2CO_3 as additive on direct reduction of boron-bearing magnetite concentrate. *J. Iron Steel Res. Int.* **2016**, *23*, 103–108. [CrossRef]
12. Zhang, S.H.; Rao, M.J.; Xiao, R.D.; You, J.X.; Li, G.H. Beneficiation of Nb and Ti carbides from pyrochlore ore via carbothermic reduction followed by magnetic separation. *Miner. Eng.* **2022**, *180*, 107492. [CrossRef]
13. Yang, S.T.; Zhou, M.; Jiang, T.; Wang, Y.-J.; Xue, X.-X. Effect of basicity on sintering behavior of low-titanium vanadium−titanium magnetite. *Trans. Nonferr. Met. Soc. China* **2015**, *25*, 2087–2094. [CrossRef]
14. Sui, Y.L.; Guo, Y.F.; Jiang, T.; Qiu, G.-Z. Separation and recovery of iron and titanium from oxidized vanadium titano-magnetite by gas-based reduction roasting and magnetic separation. *J. Mater. Res. Technol.* **2019**, *8*, 3036–3043. [CrossRef]
15. Jena, M.S.; Tripathy, H.K.; Mohanty, J.K.; Mohanty, J.N.; Das, S.K.; Reddy, P.S.R. Roasting followed by magnetic separation: A process for beneficiation of titano-magnetite ore. *Sep. Sci. Technol.* **2015**, *50*, 1221–1229. [CrossRef]
16. Chen, Y.; Williams, J.S.; Ninham, B. Mechanochemical reactions of ilmenite with different additives. *Colloids Surf. A Phys. Eng. Asp.* **1997**, *129–130*, 61–66. [CrossRef]

17. Ding, W.; Xiao, J.H.; Peng, Y.; Shen, S.-Y.; Chen, T. Iron extraction from red mud using roasting with sodium salt. *Miner. Process. Extr. Met. Rev.* **2019**, *3*, 153–161.
18. Gao, E.X.; Sun, T.C.; Liu, Z.G.; Geng, C.; Xu, C.-Y. Effect of sodium sulfate on direct reduction of beach titanomagnetite for separation of iron and titanium. *J. Iron Steel Res. Int.* **2016**, *23*, 428–433. [CrossRef]
19. Yao, G.Z.; Li, Y.L.; Guo, Q.; Qi, T.; Guo, Z.C. Preparation of reduced iron powder for powder metallurgy from magnetite concentrate by direct reduction and wet magnetic separation. *Powder Technol.* **2021**, *392*, 344–355. [CrossRef]
20. Agrawal, S.; Dhawan, N. Microwave acid baking of red mud for extraction of titanium and scandium values. *Hydrometallurgy* **2021**, *204*, 105704. [CrossRef]
21. Bian, Z.Z.; Feng, Y.L.; Li, H.R.; Wu, H. Efficient separation of vanadium, titanium, and iron from vanadium-bearing titano-magnetite by pressurized pyrolysis of ammonium chloride-acid leaching-solvent extraction process. *Sep. Purif. Technol.* **2021**, *255*, 117169. [CrossRef]
22. Chen, J.W.; Jiao, Y.; Wang, X.D. Thermodynamic studies on gas-based reduction of vanadium titano-magnetite pellets. *Int. J. Miner. Metall. Mater.* **2019**, *26*, 822. [CrossRef]
23. Liu, S.S.; Guo, Y.F.; Qiu, G.Z.; Jiang, T.; Chen, F. Solid-state reduction kinetics and mechanism of pre-oxidized vanadiumítitanium magnetite concentrate. *Trans. Nonferr. Met. Soc. China* **2014**, *24*, 3372–3377. [CrossRef]
24. Geng, C.; Sun, T.C.; Ma, Y.W.; Xu, C.-Y.; Yang, H.-F. Effects of embedding direct reduction follow by magnetic separation on recovering titanium and iron of beach titanomagnetite concentrate. *J. Iron Steel Res. Int.* **2017**, *24*, 156–164. [CrossRef]
25. Lv, X.D.; Hou, Y.L.; Xin, Y.T.; Lv, X.W. Using Na_2CO_3 as an additive to enhance the growth kinetics of iron grains during carbo-thermic reduction of ilmenite concentrate. *Powder Technol.* **2022**, *406*, 117592. [CrossRef]
26. Wu, S.C.; Li, Z.Y.; Sun, T.C.; Lu, S.X.; Cao, Z.M. Individual enrichment of titanium and iron from low-titanium beach titanomagnetite via preconcentration-reduction roasting and magnetic separation with calcium fluoride. *Powder Technol.* **2022**, *409*, 117810. [CrossRef]
27. Li, W.B.; Liu, X.; Liu, D.Q.; Han, Y.X. Mineralogical reconstruction of Titanium-Vanadium hematite and magnetic separation mechanism of titanium and iron minerals. *Adv. Powder Technol.* **2022**, *33*, 103408. [CrossRef]
28. Li, G.H.; Liu, M.X.; Rao, M.J.; Jiang, T.; Zhuang, J.Q.; Zhang, Y.B. Stepwise extraction of valuable components from red mud based on reductive roasting with sodium salts. *J. Hazard. Mater.* **2014**, *280*, 774–780. [CrossRef]
29. Han, Y.; Kim, S.; Go, B.; Lee, S.; Park, S.; Joen, H.-S. Optimized magnetic separation for efficient recovery of V and Ti enriched concentrates from vanadium-titanium magnetite ore: Effect of grinding and magnetic intensity. *Powder Technol.* **2021**, *391*, 282–291. [CrossRef]
30. Chen, P.; Hou, P.P.; Zhai, J.H.; Sun, W. A novel method for the comprehensive utilization of iron and titanium resources from a refractory ore. *Sep. Purif. Technol.* **2019**, *226*, 1–7. [CrossRef]
31. Jin, D.; Sun, R.F.; Wang, G.Y.; Deng, J.S.; Zhang, X. Flotation separation of fluorite and calcite using anhydrous glucose and aluminum sulfate as a combined depressant. *Appl. Surf. Sci.* **2023**, *624*, 157089. [CrossRef]